INTERNATIONAL JOURNAL OF ENERGY STUDIES

e-ISSN: 2717-7513 (ONLINE); homepage: https://dergipark.org.tr/en/pub/ijes

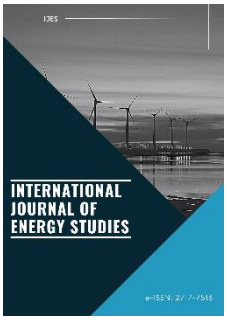

Research Article

Int J Energy Studies 2026; 11(1): 751-776

DOI: 10.58559/ijes.1781429

Received : 10 Sep 2025

Revised : 18 Dec 2025

Accepted : 26 Dec 2025

Numerical investigation on aerodynamics of NACA 4412 under wavy ground

Mehmet Bakırcı[a*], Muhammad Islam[b]

[a]*Karabuk University TOBB Technical Sciences Vocational School, ORCID: 0000-0002-1061-698X*

[b]*Karabuk University Mechanical Engineering student, ORCID: 0009-0000-4499-0999*

*(*Corresponding Author: mehmetbakirci@karabuk.edu.tr)*

Highlights

- Maximum lift occurs at the wave crest, while the minimum is observed at the trough
- Increasing angle of attack results in higher lift, drag and moment
- Different Angle of Attack (AOA) result in different aerodynamics coefficient fluctuations
- Larger wave amplitude leads to greater fluctuations in lift, drag, and moment
- Increasing ground clearance reduces the level of fluctuation
- A longer wavelength of the wavy surface decreases fluctuation

You can cite this article as: Bakırcı M, Islam M. Numerical investigation on aerodynamics of NACA 4412 under wavy ground. Int J Energy Studies 2026; 11(1): 751-776.

ABSTRACT

Improving knowledge of aerodynamic effects of wavy ground is essential especially for the development of stability and control strategies, for design improvements in the wider application of ground-effect aircraft such as ekranoplans, seaplanes and airfish-8. In this study, the aerodynamic (lift, drag and pitching moment) behavior of NACA 4412 airfoil under the effect of wavy ground was investigated with URANS CFD. The effects of different angles of attack, wavelengths, wave amplitudes and ground clearance were analyzed. While the airfoil was kept in a fixed position, wave motion in sinusoidal form was defined at the lower boundary and calculations were made by sliding mesh method. The results obtained revealed that at high angles of attack, the aerodynamic coefficients (C_L, C_D, C_M) became more sensitive to the wave parameters and the periodic fluctuations increased. Higher oscillations in lift and drag forces and moment have been observed, especially in short wavelength, high wave amplitude, and low ground clearance configurations. In addition, optimal parameter combinations are also proposed to improve aerodynamic performance in wavy ground conditions.

Keywords: Wavy ground, NACA 4412, URANS, CFD, Lift, Drag, Moment, Fluctuation, β metric

1. INTRODUCTION

Ground effect is an important research topic in the field of aeronautical engineering and has critical effects on the aerodynamic performance of Wing-in-Ground (WIG) vehicles and aircraft operating at low altitudes. Although the ground effect on traditionally flat surfaces has been studied extensively, wavy ground conditions encountered in real-life conditions have received increasing attention in recent years. These studies hold significant importance, particularly for WIG vehicles operating above the sea surface and for aircraft during landing and takeoff under unfavorable (high waves or sea roughness for WIG vehicles) weather conditions.

The vast majority of airfoil studies are carried out under free-flow and flat ground conditions, neglecting the wave effect on the ground. Ground effect is an aerodynamic phenomenon characterized by an increase in lift and a decrease in drag force when aircraft fly close to such surfaces [1]. However, in real-world scenarios such as ekranoplan (Wing in Ground effect - WIG) vehicles, air-cushioned vehicles, unmanned aerial vehicles (UAVs) traveling close to the sea surface, and certain short take-off/landing systems, aircraft interact closely with uneven, wavy ground or wavy water surfaces.

The behavior of aerodynamic forces in wavy surface conditions differs significantly from that in flat surface conditions. A study by [2] revealed that WIG vehicles flying on wavy surfaces experience periodic fluctuations in their aerodynamic coefficients, and these fluctuations create a dynamic effect depending on the surface shape. Similarly, in the research conducted by [3], it was determined that in the analyses conducted on the NACA 4412 airfoil, fluctuation amplitudes exceeding 100% were observed in the lift coefficient under wavy surface conditions, and this situation could create serious stability problems, especially at the 0° angle of attack.

The effect of wavy surface parameters on lift characteristics involves the complex interplay of factors such as AOA, wave amplitude, wavelength and ground clearance. In the study conducted by [4] on the NACA 4412 profile, it was shown that increasing the wave amplitude from 0.05c to 0.1c, with 'c' being the airfoil chord length, creates significant periodic oscillations in the lift coefficient and can cause sudden lift drops and even negative lift values at low angles of attack (0° and 1°). This poses a critical danger to the stability and safety of WIG vehicles. On the other hand, when the wave crest approaches the leading edge of the wing at relatively higher angles of attack (2° and 4°), an increase in time-average lift values is observed due to the compression of air under the wing.

A study by [5] on a controlled airfoil (usually performed by blowing high-pressure jet air from areas near the trailing edge of the wing to achieve high lift) revealed that lift augmentation is

possible with blowing control in wavy water surface conditions. But this control also magnifies unstable fluctuations. In the study, it was found that larger wave amplitude and longer wavelengths cause more lift fluctuations.

The effects of wavy surface conditions on drag and moment characteristics are not as dramatic as lift, but they have significant operational implications. In the study of [6], it is stated that as the flight altitude decreases, the drag coefficient increases and the nose-down (pitching) moment coefficient becomes more negative, which reduces stability. In the comparative study conducted by [7], it was determined that drag increase in fixed ground conditions was due to boundary layer thickening problems, while drag decrease was observed in moving ground conditions.

A BiGlobal (a linear stability analysis technique used in CFD to study how small disturbances that vary in two spatial directions but are homogeneous in the third direction develop in two-dimensional bottom flows) stability analysis study by [8] on a NACA 4415 airfoil showed that increasing the amplitude of a wavy surface results in an increase in the lift coefficient while keeping the average airfoil-to-ground distance constant. This suggests that the pressure buildup under the wing is consistent with classical ground effect behavior.

Various CFD methodologies have been developed and applied for aerodynamic analyses in wavy surface conditions. In the study carried out by [6] using Ansys Fluent and Spalart-Allmaras turbulence model, the relative motion between the wing and the wavy surface was modeled with the sliding mesh technique and more realistic simulations of unstable ground effect aerodynamics were obtained. The URANS equations, validated using experimental data in [3] provide an effective approach for the analysis of wavy surface effects over a wide range of angles of attack (0°-18°).

In the study of [5], the overset grid approach (a meshing technique in which grid blocks are superimposed) and the Volume of Fluid (VOF) method (a numerical scheme for tracking phase boundaries in multiphase flows such as air–water) were combined to investigate wavy water-surface conditions with circulation control (typically implemented by blowing high-pressure jet air from regions near the wing's trailing edge to enhance lift). Using this approach, the aerodynamic behavior of the airfoil was successfully modeled. [9] used the discrete vortex method (a potential flow-based numerical method that estimates the lift and flow field by time-dependent monitoring of free vortices in the flow) and time-domain Green's function (an integral solution-based method that calculates the system response to a stimulus in acoustic, hydrodynamic, or aerodynamic systems using time-dependent green functions). Their non-linear, two-dimensional

unsteady analysis provides an alternative methodology for studying the effect of WIG on water waves.

Various approaches have been developed to optimize aerodynamic performance in wavy surface conditions. Performance optimization of the NACA 4412 profile was performed by [10] using the "full factorial design of experiments (DOE)" methodology using full experimental design parameters, and a validated model was developed for the interactions between ground distance and angle of attack. In the study, it was found that low ground distance significantly improved lift performance, but increasing ground distance or angle of attack caused a decrease in lift efficiency.

The flight control strategies developed by [11] for WIG vehicles aim to improve fuel efficiency by minimizing geometric flight altitude over wavy sea surfaces. The study showed that optimal performance can be achieved between rigid altitude stabilization and full use of the self-stabilizing features of WIG vehicles. Furthermore, the findings reveal that significant fuel savings are achieved but only in large WIG vehicles with wing chord significantly larger than wave height.

The effects of wavy surface conditions on aerodynamic stability are critical, especially for WIG vehicles and low-altitude operations. [12] extensive literature review reveals the challenges encountered in longitudinal and lateral attitude stabilization of WIG tools and how they grow in unstable phases such as takeoff, in-flight movement, and landing. In particular, it is emphasized that ground proximity and wave-induced disturbances magnify pitch, heave, roll, yaw instabilities and that effective attitude control (ensuring that it remains stable and reaches the desired directions quickly and precisely) is necessary to maintain lift consistency and stable flight paths.

Although ground effect on flat ground has been extensively studied in the existing literature, further studies are needed to better understand the aerodynamic behavior on undulating ground. In particular, the effects of parameters such as wavelength (λ), wave amplitude (a), flight altitude (h) and angle of attack (AOA, α) on the lift, drag and moment characteristics of the airfoil, periodic load changes and instability effects resulting from the time-dependent nature of the flow, unsteady fluctuations of coefficients such as C_L, C_D and C_M and the possible consequences of all these effects on ekranoplan stability, energy consumption and safety have been addressed only in a limited number of studies in the literature, and these studies are mostly theoretical approaches or simplified 2D models. Although previous studies have numerically examined wavy ground effects on the NACA 4412 profile [13]and compared flat and wavy ground behavior [14], the combined dynamic effects of various wave parameters, ground clearance, and angles of attack, together, on aerodynamic performance have not yet been investigated in sufficient detail.

The main objective of this study is to fill this important gap in the literature by comprehensively examining the aerodynamic performance of an airfoil under the influence of wavy ground. The originality of the study is the unsteady examination of the wavy ground effect with 2D URANS analysis, and the detailed comparison of the changes in lift, drag and moment coefficients at different wavelengths, amplitudes, ground clearness and angles of attack. It is hoped that these comprehensive analyses will shed light on situations such as instability, oscillation and performance degradation for realistic flight scenarios, and will serve as a critical reference study in terms of both optimizing the design criteria of ground-effect aircraft and developing control strategies in new generation unmanned systems.

2. METHODOLOGY

In this study, how angle of attack, height from the ground (water) surface, wavelength and amplitude-different parameters- affect the lift, drag and moment values formed in the airfoil according to time was analyzed with CFD and interpreted with column graphs. The time-varying behavior of lift (C_L), drag (C_D) and moment (C_M) coefficients was analyzed in 16 scenarios based on different angles of attack (0° and 8°), ground clearance (h/c; 0.4 and 0.8), wavelength (λ/c; 1 and 3) and wave amplitude (a/c; 0.07 and 0.2). Different wavelengths (λ/c) and wave amplitudes (a/c) were determined as variable parameters in order to fully understand the effects of the wavy surface on the aerodynamic flow structure and pressure distribution Following the experimental setup of [15], the chord length (c) was set to 0.15 m and freestream velocity was 30.8 m/s. This comprehensive approach aims to reveal the dynamic aerodynamic behavior of aircraft under the influence of WIG under wavy surface conditions.

2.1. Aerodynamic Coefficients

It is analyzed that how the lift, drag and moment coefficient values formed in the airfoil on wavy ground changed throughout the wave and according to different parameters. As aerodynamic coefficients, lift, drag and moment values were calculated with equations 1, 2, 3, 4, 5, and 6.

$$C_l = \frac{L}{\frac{1}{2}\rho V^2 A} \quad (1)$$

$$C_d = \frac{\mathrm{D}}{\frac{1}{2}\rho V^2 A} \quad (2)$$

$$C_m = \frac{M}{\frac{1}{2}\rho V^2 Ac} \quad (3)$$

Average lift coefficient:

$$C_L = \frac{1}{T}\int_0^T C_L\,(t)dt \quad (4)$$

Average drag coefficient:

$$C_D = \frac{1}{T}\int_0^T C_D(t)dt \quad (5)$$

Average moment coefficient:

$$C_M = \frac{1}{T}\int_0^T C_M\,(t)dt \quad (6)$$

In this study, as shown in Figure 1, four different wave geometries were used, the different wavelengths are λ=1c and λ=3c, and the different wave amplitude are a=0.07c and a=0.2c.

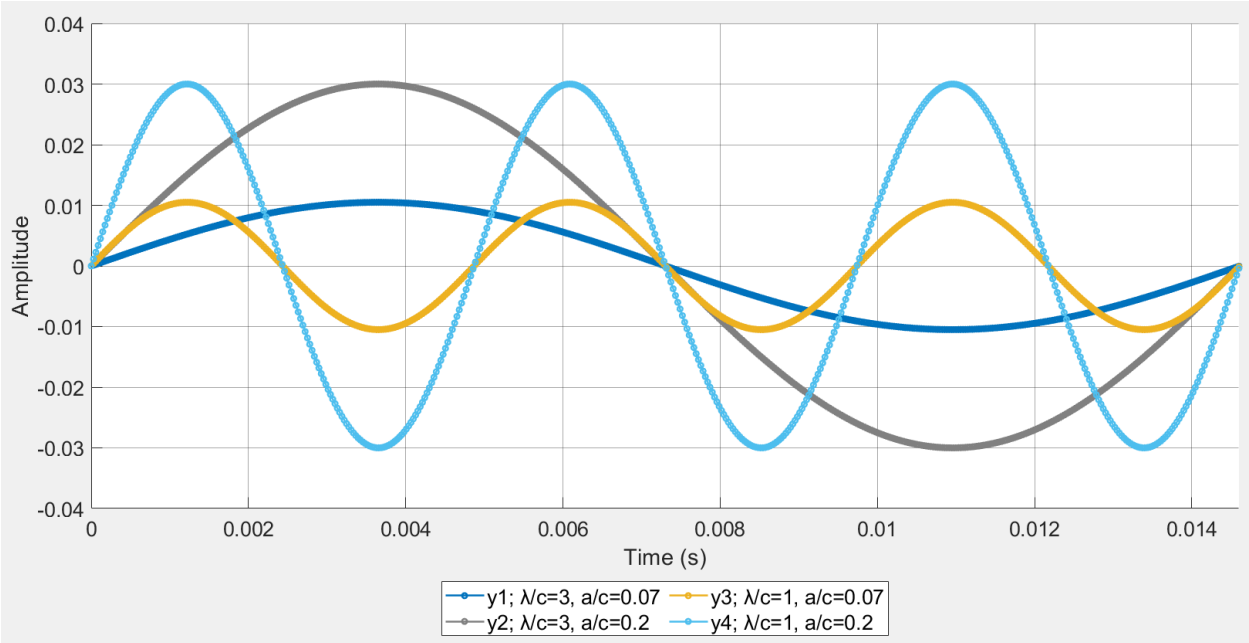

Figure 1. Sinusoidal wave profiles used in the study for different wavelength (λ/c) and amplitude (a/c) ratios: (a) λ/c=1, a/c=0.07; (b) λ/c=1, a/c=0.2; (c) λ/c=3, a/c=0.07; (d) λ/c=3, a/c=0.2 (Amplitude is in meter)

The aerodynamic coefficients of lift, drag and moment for an airfoil under the effect of wavy ground were calculated by CFD. In the analyses, the airfoil was positioned at a certain distance from the surface of the water. Different angles of attack, airfoil velocity, and ground clearance above the surface were parametrically studied to accurately study the aerodynamic effect of wave motion. The wave surface was constructed using a sinusoidal wave model, and wavelength (λ) and wave amplitude (a) were defined as variable parameters. In this way, the temporal effects of wave geometry on the C_L, C_D and C_M on the airfoil were systematically investigated.

2.2. CFD analysis

The CFD calculation region was divided into two main domains, the upper and the lower, as shown in Figure 2. The upper region contains the airfoil and the surrounding air environment. In this zone, a speed inlet and a pressure outlet are defined to determine the initial conditions of the flow. For upper boundary of the calculation area, Far-field boundary was used. The lower region represents the water region where the wave movement will be created and the sliding mesh method is used. In order to accurately simulate the interaction of the airfoil with the waves, an interface is defined between the upper and lower regions. The velocity inlet limit of the subregion is determined to be equal to the speed at which the wave travels.

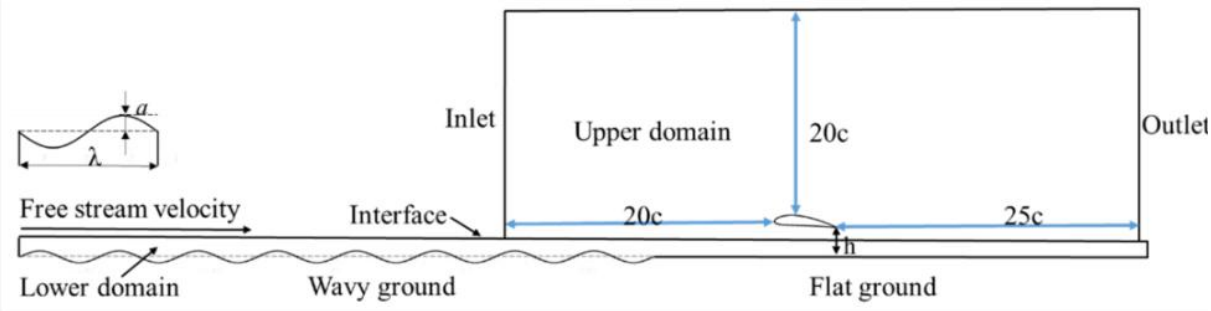

Figure 2. Computational domain and boundary conditions for the airfoil moving over a wavy ground, adapted from [3]

A proper meshing strategy is adopted for the accuracy and efficiency of calculations. A condensed mesh was used in areas with high flow gradients around the airfoil (Figure 3).

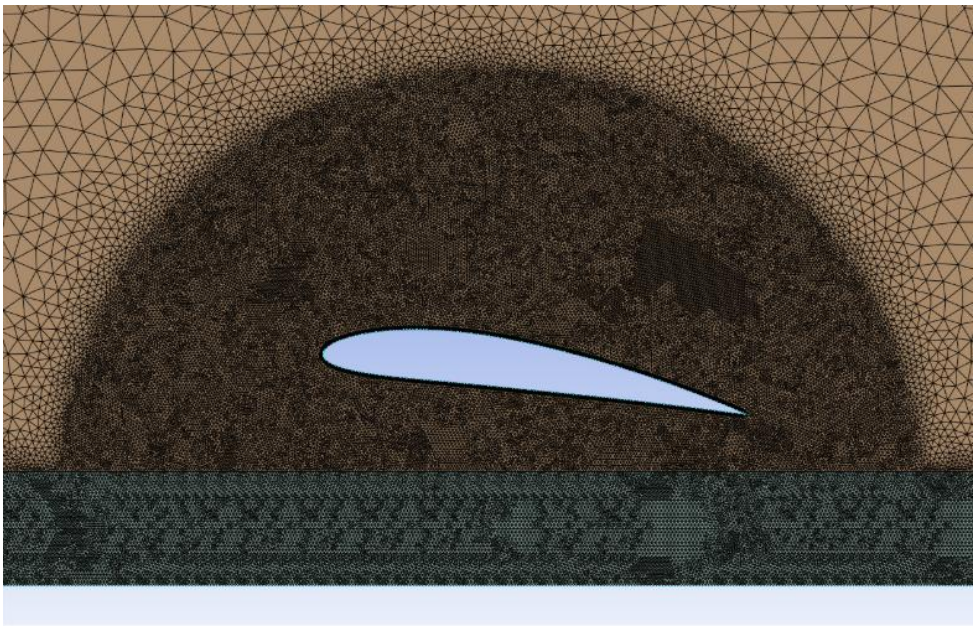

Figure 3. Close-up view of the refined C-type mesh around the NACA 4412 airfoil, showing the boundary layer resolution.

For this analysis, a two-dimensional computational domain was meshed using a triangular cell structure. The use of triangular elements was preferred because the combined complexity of the airfoil geometry and the wavy surface, along with the application of a sliding mesh for unsteady moving ground conditions, makes quadrilateral cells less practical. Additional considerations such as mesh accuracy and computational cost further supported this choice. The airfoil geometry and wave motion were modeled using a sliding mesh technique in the lower part of the domain. To assess solution accuracy and ensure grid independence, a mesh independence study was performed by testing different mesh densities, the SST k–ω model was employed. In accordance with the requirements of this model, the first cell height (y+) adjacent to both the airfoil and the wavy ground surface was set to approximately $y^{+}\approx1$ (Figure 3).

Ensuring temporal convergence is of great importance for Unsteady CFD analysis. Therefore, the time step (Δt) was determined so that the CFL number; CFL≤1 is determined. The optimum Δt value was selected using the relation $\Delta t=(\lambda/V)(CFL)$ depending on the wave period ($T=\lambda/V$). At each time step, solution convergence was achieved by continuing iterations for the momentum and turbulence equations until their residual errors were less than 10^{-6}. As a turbulence model, the SST k−ω model was preferred because it offers fast and reliable solutions.

Reynolds number of 314,285 and a ground clearance of 0.15, according to the reference experimental [15] conditions. The main objective of the study is to provide accurate estimation of

lift (C_L), drag (C_D) coefficients at both 0° and 8° angles of attack using various mesh structures and turbulence models.

Mesh Optimization and Grid Precision Review: Five different grid configurations (Grid A, B, C1, C2, and D) were compared for their C_L and C_D accuracies, wall convergence (y^+) values, CFL stability, and computational efficiencies to evaluate mesh accuracy and grid precision:

- **Grid A:** SST k-ω model was used. The coarsest mesh; ($\Delta x_{max} = (7.0)10^{-4}$ m), with $y^+ = 2.8$ and CFL = 7, $C_L = 0.305$ with an 18.2% deviation from experimental C_L and $C_D = 0.0158$ with a 97.5% deviation from experimental C_D.
- **Grid B:** SST k-ω model was used. A more refined mesh; ($\Delta x_{max} = (5.0)10^{-4}$ m). With $y^+ = 2.8$ and CFL = 1.38, $C_L = 0.339$ (9.1% error) and $C_D = 0.0158$ (97.5% error). Despite the high error rate in drag coefficient but minimum error of C_L, therefore this grid was preferred for later stages.
- **Grid C1:** SAS model was used with a finer mesh; ($\Delta x \approx (3.5)10^{-4}$ m). The SAS model is a hybrid CFD turbulence model that adapts to local flow scales in turbulent regions of the flow by combining the advantages of RANS and LES methods. However, significant errors were observed, such as 39.4% in the C_L estimation and 86.3% in the C_D estimate. The y^+ and CFL values could not be controlled, indicating that the SAS model did not accurately reflect the lift characteristics.
- **Grid C2:** SST k-ω model was used. It is a fairly fine mesh; ($\Delta x \approx (3.5)10^{-4}$ m), $y^+ = 1.34$ and CFL = 1.36. C_L error was recorded as 9.7% and C_D was recorded as 87.5%. Although the lifting accuracy is similar to Grid B, the calculation cost is higher.
- **Grid D:** SST k-ω model was used. It is the grid with the highest resolution; ($\Delta x \approx (2.5)10^{-4}$ m), $y^+ = 0.96$, and CFL = 1.11 yielded the lowest drag error ($C_D = 0.0142$) with 77.5% error, although the value of C_L was not specified. However, the increased computational load of this grid did not justify the marginal benefits it provided over Grid B.

Simulations performed at an 8° AOA using Grid B showed a low error of only 2%, with a value of $C_L = 1.265$ compared to the experimental C_L (1.291). The estimated C_D (0.0185) resulted in an error rate of 17.8% compared to the experimental C_D (0.0157). This error rate reflects the sensitivity of the drag estimates to the turbulence model and grid resolution and is evaluated within acceptable limits.

In all steady and unsteady analyses, the SST k-ω turbulence model was adopted. This model has been deemed superior due to its ability to accurately model boundary layer behaviors, separations,

and reverse pressure gradients. In contrast, the SAS model was inadequate in predicting the lift force. In order to resolve the viscous sublayer correctly and to avoid the need for wall functions, time step and grid controls were performed in all simulations by providing the conditions CFL < 1.5 and $y^+ < 3$.

Among all the mesh configurations, Grid B is selected as the most suitable solution with high lifting accuracy, acceptable drag error, numerical stability (CFL ≈ 1.38) and favorable wall convergence ($y^+ \approx 2.8$). The SST k-ω turbulence model yielded more successful results compared to the SAS model with its reliable predictive performance in boundary layer and separation zones. Relatively high error rates in drag estimates should be interpreted within the constraints inherent in CFDs, and the results obtained should be considered valid and reliable. This validated configuration (Grid B + SST k-ω) provides a robust foundation for unsteady aerodynamic analyses of the ground effect, such as 2D unsteady CFD's with NACA 4412 airfoils, sliding mesh, moving walls and SST k-ω analyses on wavy ground. The results are summarized in Table 1.

Based on the CFD analysis results, C_L, C_D and C_M coefficients were calculated for different angles of attack, ground clearance, and wave parameters. Validation was performed by comparing the lift and drag coefficient values obtained with the current operating setup the ground effect on flat surface for h/c=0.4 and 0.8 and AOA values of 0° and 8° with the [15]. The results are given in Table 2.

Table 1. Grid independence test for flat ground, h/c=0.15 (Verification-[15]

Grid	α	C_L (EXP.)	C_L (CFD)	Lift Error	C_D (EXP.)	C_D (CFD)	Drag Error	y^+	CFL	Turbulence Model
A	0°	0.373	0.305	18.2%	0.0080	0.0158	97.5%	2.8	7.00	SST k-ω
B	**0°**	**0.373**	**0.339**	**9.1%**	**0.0080**	**0.0158**	**97.5%**	**2.8**	**1.38**	**SST k-ω**
C1	0°	0.373	0.226	39.4%	0.0080	0.0149	86.3%	—	—	SAS
C2	0°	0.373	0.337	9.7%	0.0080	0.0150	87.5%	1.34	1.36	SST k-ω
D	0°	0.373	0.335	10%	0.0080	0.0142	77.5%	0.96	1.11	SST k-ω
B	**8°**	**1.291**	**1.265**	**2.0%**	**0.0157**	**0.0185**	**17.8%**	**2.8**	**1.38**	**SST k-ω**

In CFD analyses, drag prediction is generally more sensitive than lift prediction because drag is influenced by both pressure and viscous shear contributions of comparable magnitude, whereas lift is predominantly governed by pressure forces. Consequently, even small numerical variations can lead to noticeable discrepancies when compared to experimental data. This sensitivity is

further increased in two-dimensional simulations where flow effects across the airframe and three-dimensional vortex structures are neglected, often resulting in higher drag estimates. Additionally, since drag coefficients are generally small in magnitude, small absolute deviations can translate into relatively large percentage differences. These characteristics are well-documented in the literature and do not show any numerical discrepancies in current simulations [16, 17]. Additionally, the main objective of this study is not to find the absolute C_D values, but to examine the relative effects of different parameters on C_D and their fluctuation trends.

Table 2. Validation (Flat ground)

		Lift		Drag	
α	h/c	Present study	Experimental [15]	Present study	Experimental [15]
0°	0.4	0.368	0.448	0.016	0.008
0°	0.8	0.391	0.460	0.017	0.008
8°	0.4	1.091	1.275	0.027	0.015
8°	0.8	1.086	1.274	0.028	0.014

3. RESULTS AND DISCUSSION

The results obtained from the CFD analysis, presented through pressure contours and bar charts, illustrate the significant influence of wave's position on airfoil pressure distribution. The contours in Figure 4 and Figure 5. Figure 4 shows the airfoil at a wave crest (t*=0), while Figure 5 shows it at a wave trough (t*=0.5), for the constant parameters α=8°, λ/c=3, h/c=0.4, and a/c=0.2. At the wave crest, a maximum negative pressure (vacuum) and a maximum positive pressure occurs on the airfoil's top and bottom surfaces, respectively. This maximized pressure differential generates the highest lift force. Conversely, at the wave trough, both the negative and positive pressures are minimized, resulting in a substantially lower pressure differential and, consequently, a reduced lift force.

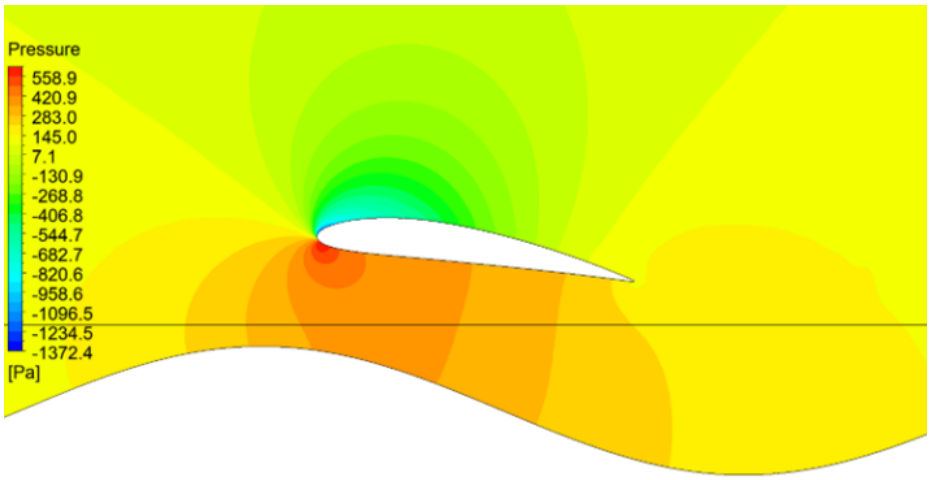

Figure 4. Pressure contour for crest (t*=0)

At wave crest the pressure varies between –1372 Pa to +559 Pa. When the airfoil approaches a wave crest, it experiences a decrease in effective altitude and a corresponding increase in its effective AOA. This combined aerodynamic effect significantly increases the pressure differential across the airfoil's surfaces. The magnitude of the negative pressure on the upper surface intensifies, creating a powerful suction force, while the positive pressure on the lower surface concurrently rises. The combined effect of these phenomena is the generation of a substantial net lift force.

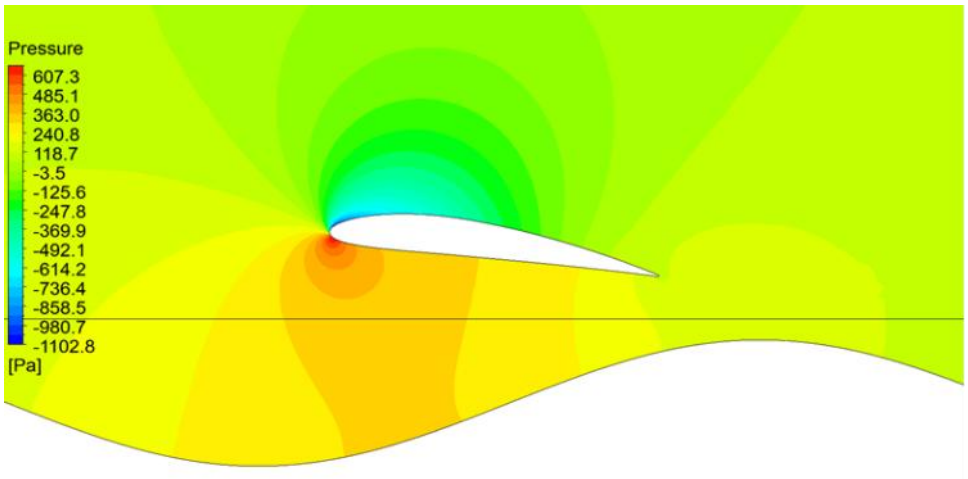

Figure 5. Pressure contour for trough (t*=0.5)

At wave trough the pressure varies between –1103 Pa to +607 Pa. When an airfoil approaches a wave trough, it experiences an increase in effective altitude, which leads to a reduction in ground effect. This is accompanied by a corresponding decrease in the effective angle of attack. The combined result of these effects is a significant reduction in the pressure difference between the

upper and lower surfaces of the airfoil compared to the wave crest. The negative pressure on the upper surface becomes less pronounced, creating a weaker suction force, and the positive pressure on the lower surface also decreases. Consequently, these phenomena result in a relatively lower net lift force.

Table 3. All cases used in this study

CASES	α	h/c	λ/c	a/c	CASES	α	h/c	λ/c	a/c
Case 1	0	0.4	1	0.07	**Case 9**	8	0.4	1	0.07
Case 2	0	0.4	1	0.2	**Case 10**	8	0.4	1	0.2
Case 3	0	0.4	3	0.07	**Case 11**	8	0.4	3	0.07
Case 4	0	0.4	3	0.2	**Case 12**	8	0.4	3	0.2
Case 5	0	0.8	1	0.07	**Case 13**	8	0.8	1	0.07
Case 6	0	0.8	1	0.2	**Case 14**	8	0.8	1	0.2
Case 7	0	0.8	3	0.07	**Case 15**	8	0.8	3	0.07
Case 8	0	0.8	3	0.2	**Case 16**	8	0.8	3	0.2

3.1. Fluctuations of Aerodynamic Coefficients

The resulting CFD results were shown in bar charts. The stability assessment was made by the analysis of the temporal fluctuations (maximum-minimum difference) of the coefficients; Larger fluctuations indicate higher instability.

Lift coefficient (C_L): Lift max, min and fluctuation values in 8 different situations for 0° angle of attack are shown in Figure 6.

The $C_{L,max}$ occur in case 8 and while the $C_{L,min}$ at case 4 for 0° angle of attack. The Cl fluctuations ($\Delta C_L = C_{L,max} - C_{L,min}$) are generally small, ranging from 0.0003 (Case 5) to 0.071 (Case 4). Larger wave amplitude (a/c=0.2) generally causes more fluctuations than smaller amplitudes (a/c=0.07). The effect of wavelength is that longer wavelengths (λ=3c) increase fluctuations (Case 04 vs Case 02) and (Case 7 vs Case 05). The largest lift fluctuation occurs in case 4 for 0°. Near the ground, large wave amplitude and large wavelength most lift fluctuations occur.

Lift max, min and fluctuation values in 8 different situations for 8° of attack angle are shown in Figure 7.

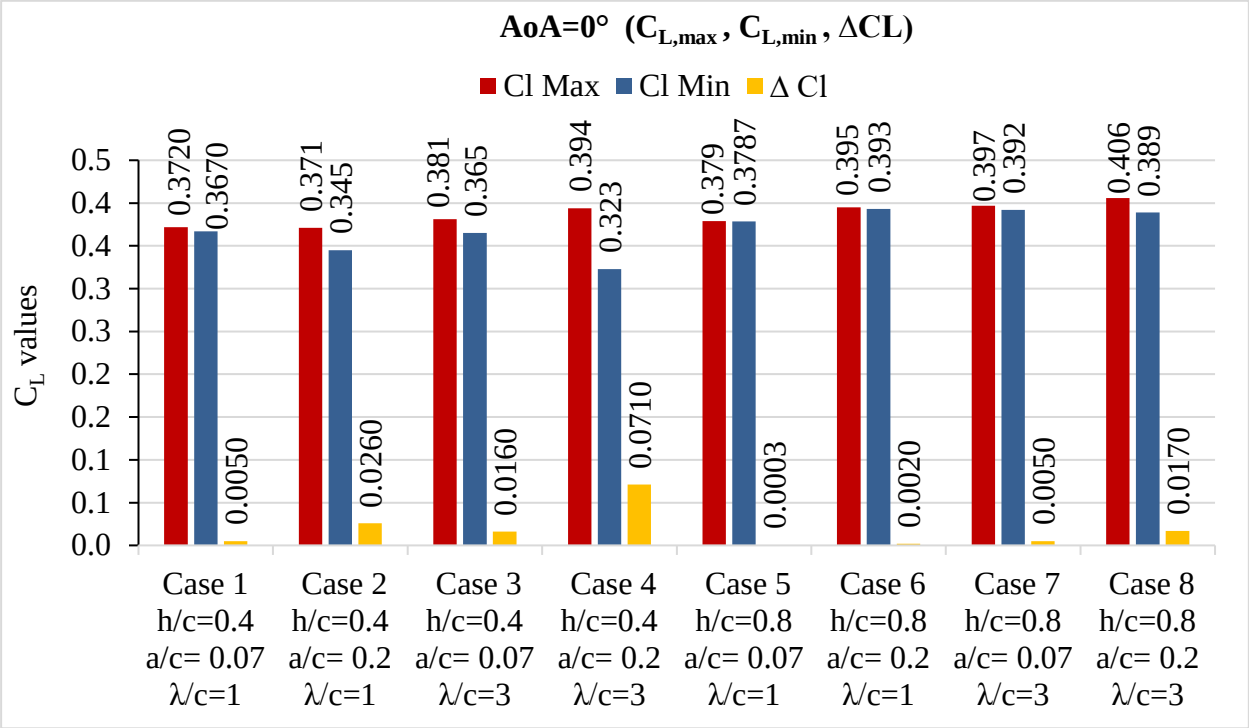

Figure 6. Comparison the lift coefficient (maximum, minimum and fluctuation) values for 0°

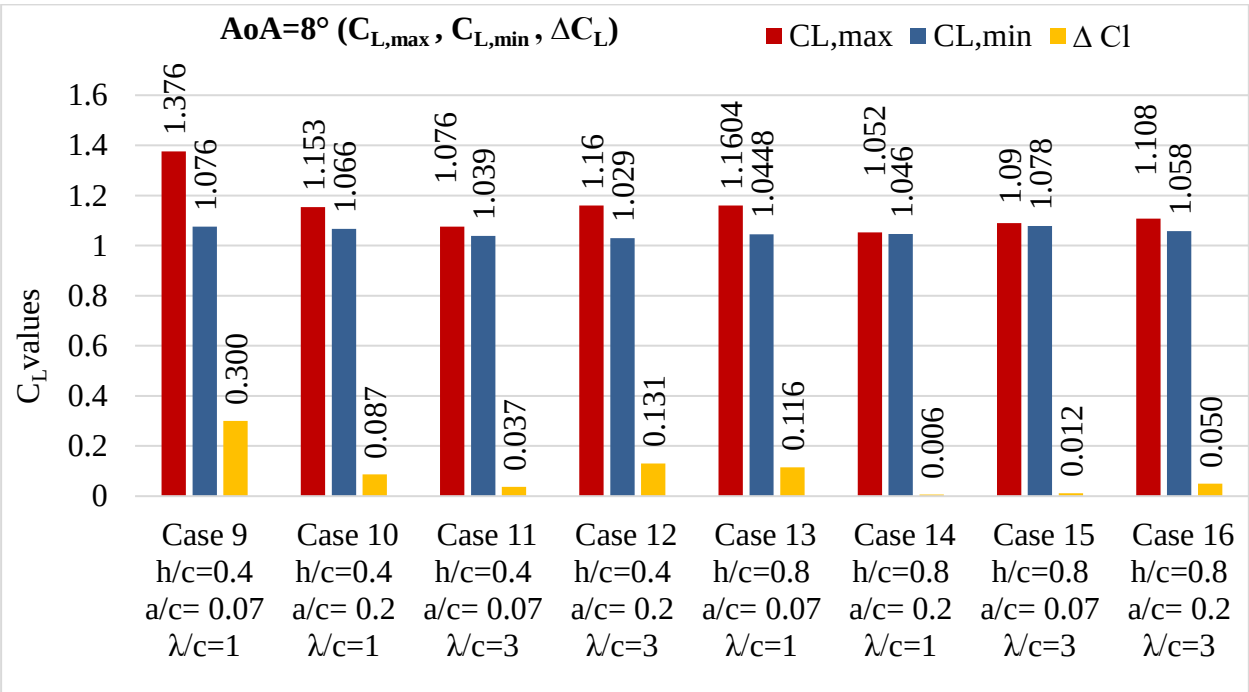

Figure 7. Comparison of C_L (maximum, minimum and difference) values for 8°

$C_{L,max}$ occurs at case 9 and while the $C_{L,min}$ at case 12 for 8° AOA. Much larger fluctuations were observed at an AOA of 8° than at 0°. For example, at 0° the maximum ΔC_L is 0.071, while in Case 9 at 8° this value goes up to 0.3. The largest lift fluctuation occurred in case 9 for 8°. Close to the

ground, smaller wavelength and smaller wave amplitude have the most lift fluctuation. In general, a higher ground clearance (h/c=0.8) tends to reduce fluctuations compared to h/c=0.4. This suggests that the airfoil is less exposed to wave action as it moves away from the surface.

Drag coefficient (C_D): The minimum, maximum and difference coefficient values of the drag coefficient at 0° angle of attack are shown in Figure 8.

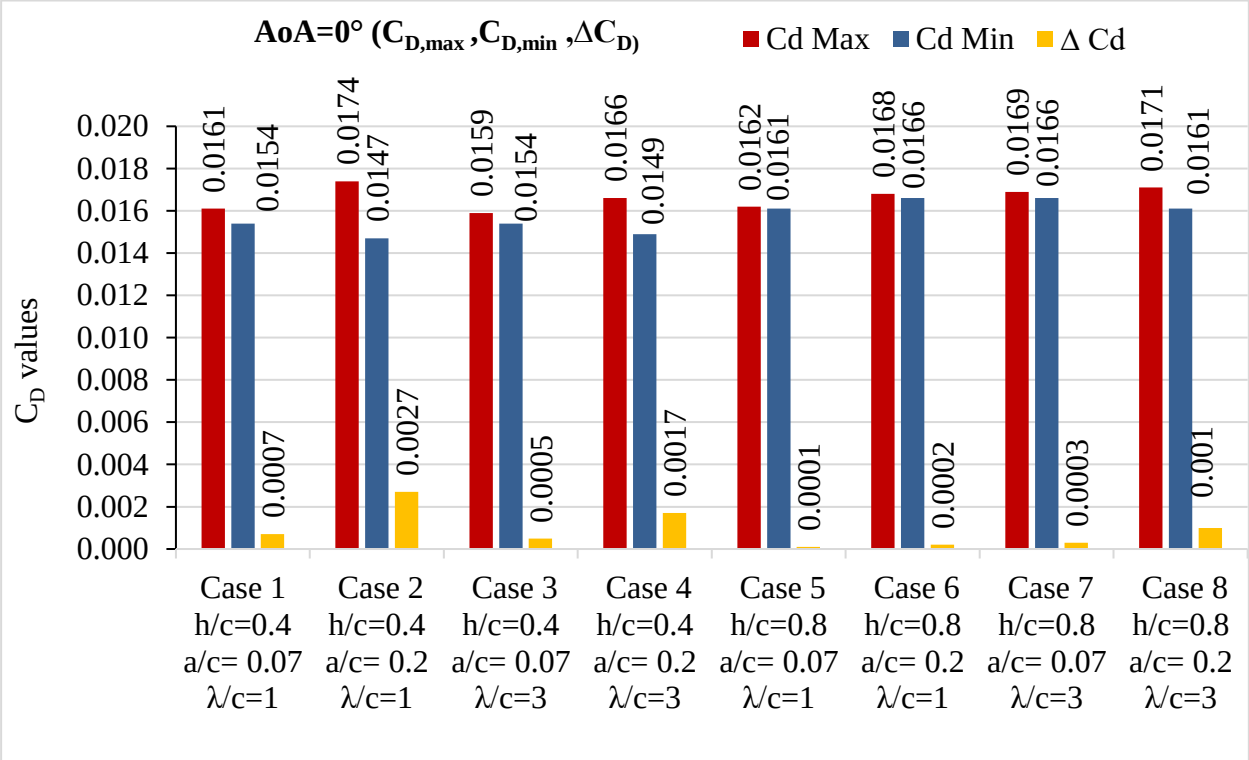

Figure 8. Comparison of C_D values (maximum, minimum and difference) for 0°

The $C_{D,max}$ occur at case 2 and $C_{D,min}$ also at case 2 for 0° angle of attack. Similarly, the largest drag change occurred in case 2 and case 4. Drag fluctuation is higher near the ground and at high wave amplitude. Wavelength is the parameter that has the least effect on drag fluctuation. The minimum drag fluctuation occurs at case 5.

The minimum, maximum and difference coefficient values of the drag coefficient at an 8°angle of attack are shown in Figure 9.

The $C_{D,max}$ occur at case 11 and while the $C_{D,min}$ at case 12 for 8° angle of attack. Similarly, the largest drag fluctuation for 8° also occurred in Case 12, while the $C_{D,min}$ occur at case 14. The high wave amplitude and large wavelength caused drag fluctuations. When these two cases were compared, more drag changes took place in the one closer to the ground.

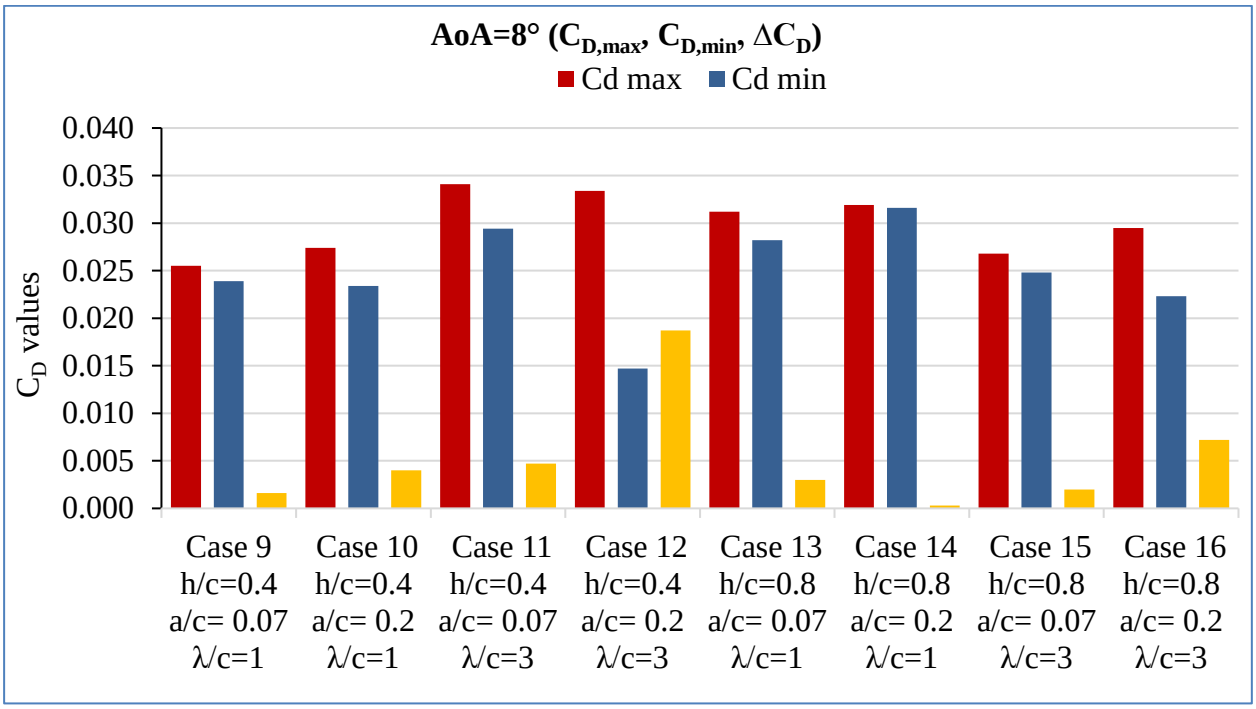

Figure 9. Comparison of drag coefficient values (maximum, minimum and difference) for 8°

Lift-Drag Ratio (C_L/C_D): The changes of the average C_L/C_D value, which is an indicator of aerodynamic performance, according to different ground clearance and wave parameters at 0° angle of attack are shown in Figure 10.

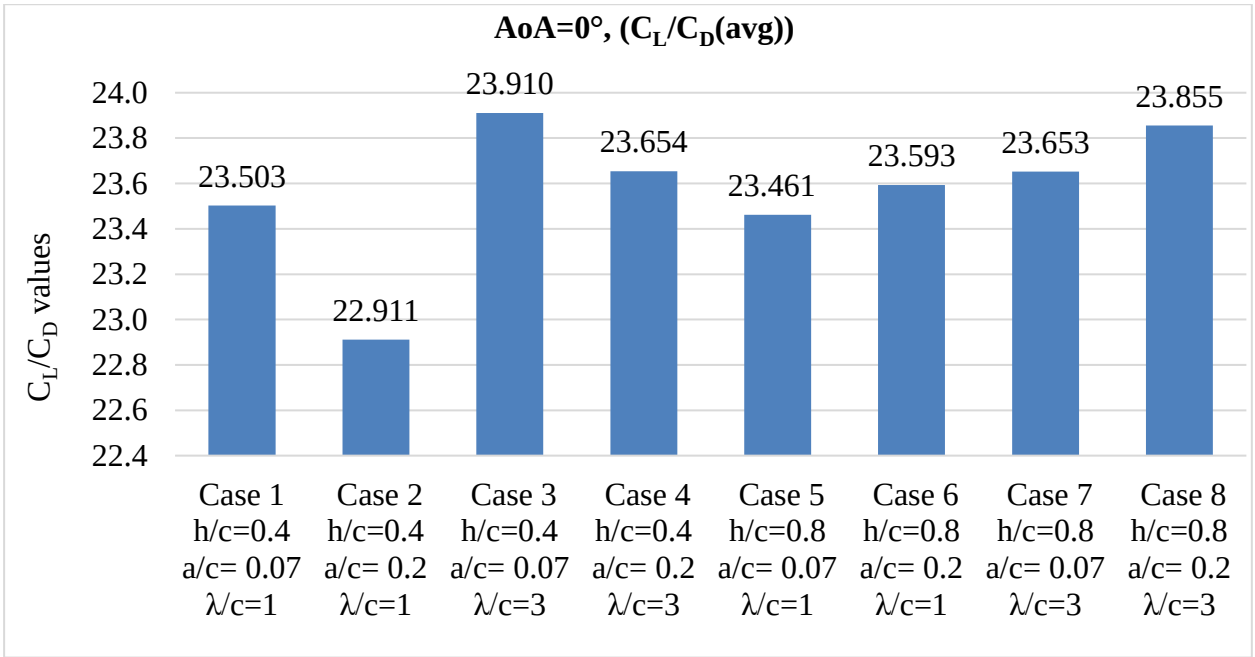

Figure 10. Average lift/drag values for 0° AOA

The highest aerodynamic efficiency was obtained in case 3 for 0° and the lowest efficiency was obtained in case 2. Near the ground, the highest aerodynamic efficiency was formed at low wave amplitude and large wavelength. High wave amplitude and small wavelength reduced aerodynamic efficiency.

The changes of the average lift/drag value with different ground clearance at 8° angle of attack and according to wave parameters are shown in Figure 11.

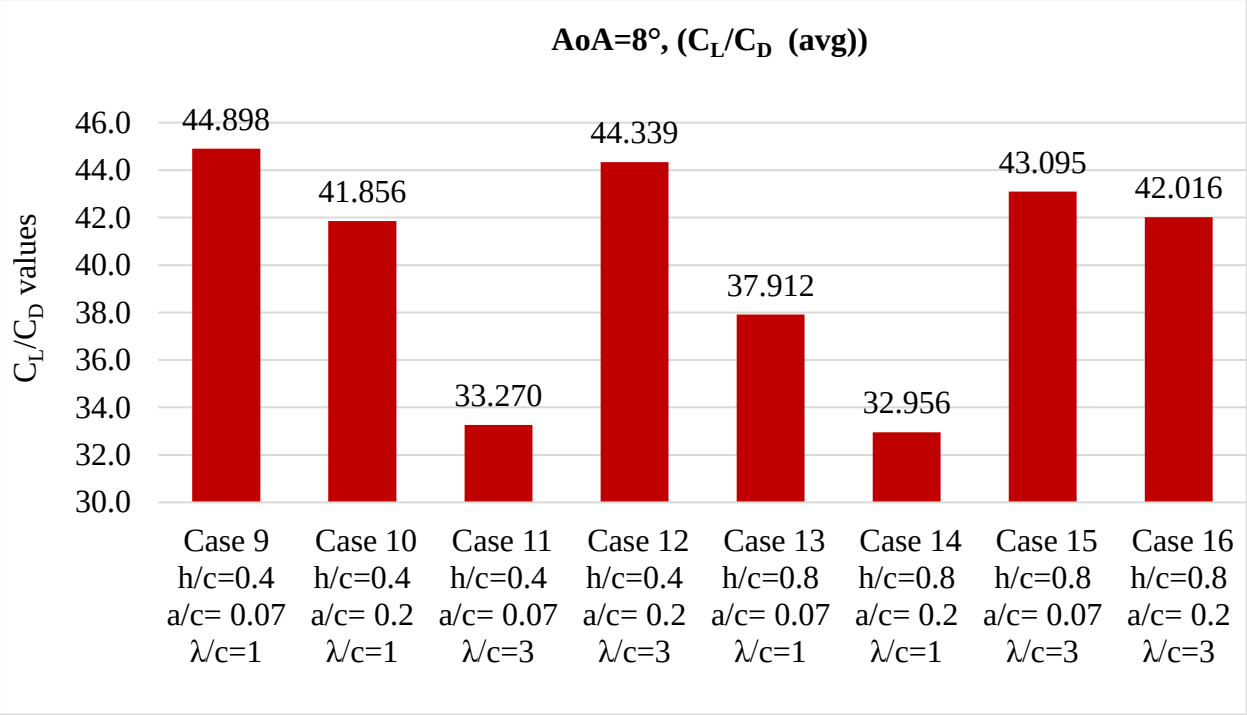

Figure 11. Lift/drag values for 8° AOA

For 8°, the average C_L/C_D value reaches its highest values in case 9 and case 12, while case 11 and case 14 have its lowest values. It seems that being close to the ground is the most important factor. However, the wave parameters also call this assessment into question. It can be said that combinations of low amplitude, long wavelength and when close to the ground and similarly high amplitude, short wavelength and when far from the ground adversely affect aerodynamic efficiency.

Moment Coefficient (C_M): The minimum and maximum C_M values at 0° angle of attack are shown in figure 12. The $C_{M,max}$ occur at case 5 while the $C_{M,min}$ occur at case 1. For 0°, it is understood that the wavelength is short and the minimum and maximum moment values are small while the airfoil is close to the ground. However, although the wavelength is short, the pitching

moment values can be large when away from the ground. The minimum and maximum values of the C_M at an angle of attack of 8° are shown in Figure 13.

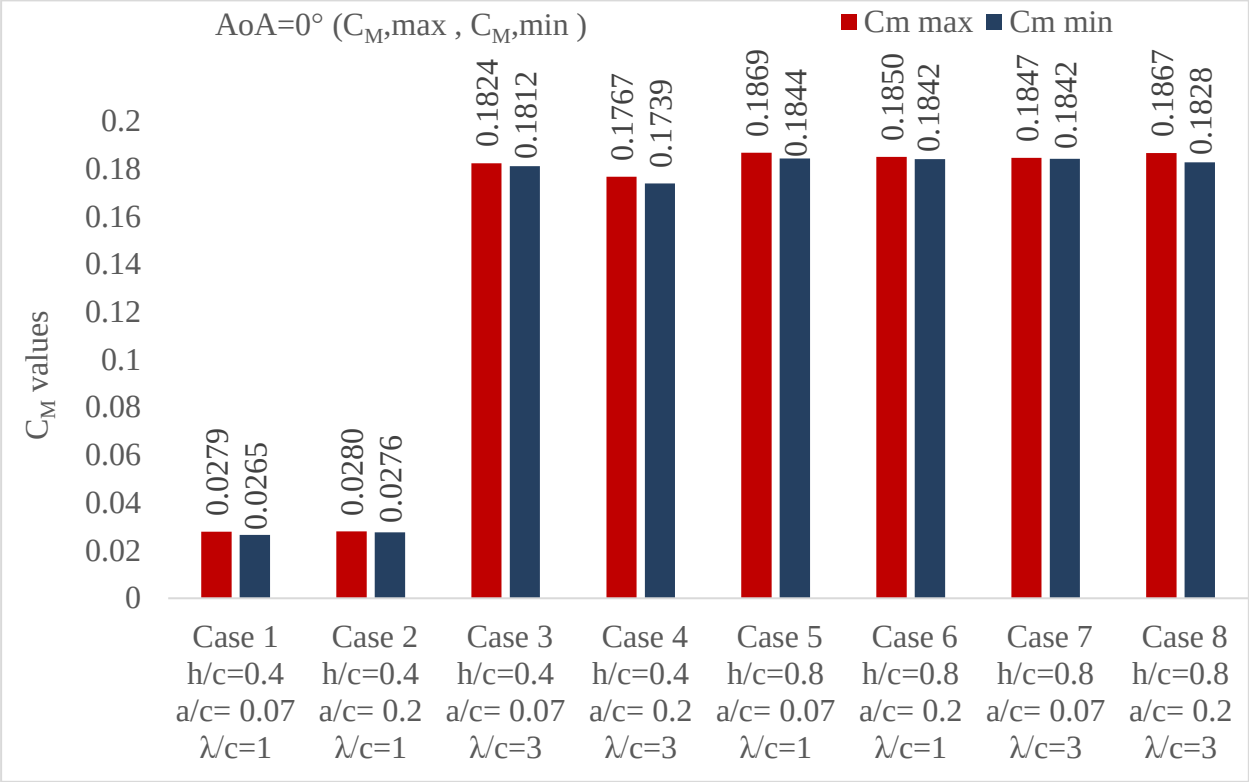

Figure 12. Comparison of C_M (min-max) values for 0°

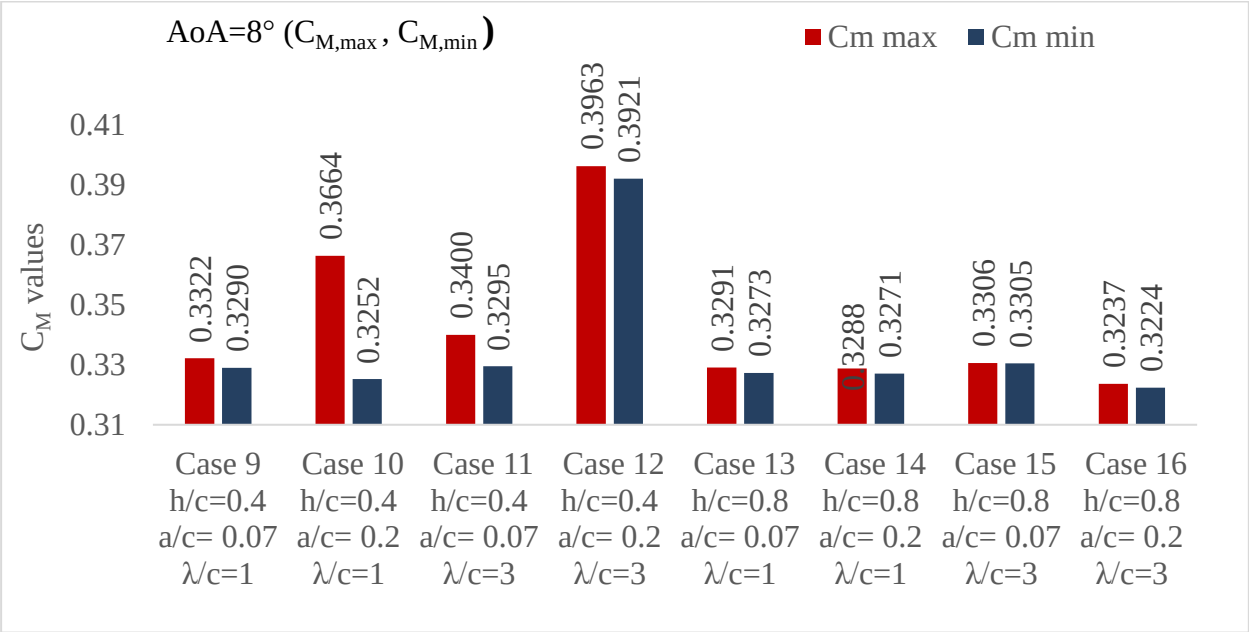

Figure 13. Comparison of C_M (min-max) values for 8°

The $C_{M,max}$ occur at case 12 while the $C_{M,min}$ occur at case 16. It can be said that the moment maximum and minimum values are not affected much by different parameters. However, case 12 reaches its highest values. It can be seen from the graphs in figure 13 that the moment values are relatively larger in the combination of large wave amplitude and long wavelength close to the ground.

The changes in moment values for both 0° and 8° are shown in Figure 14.

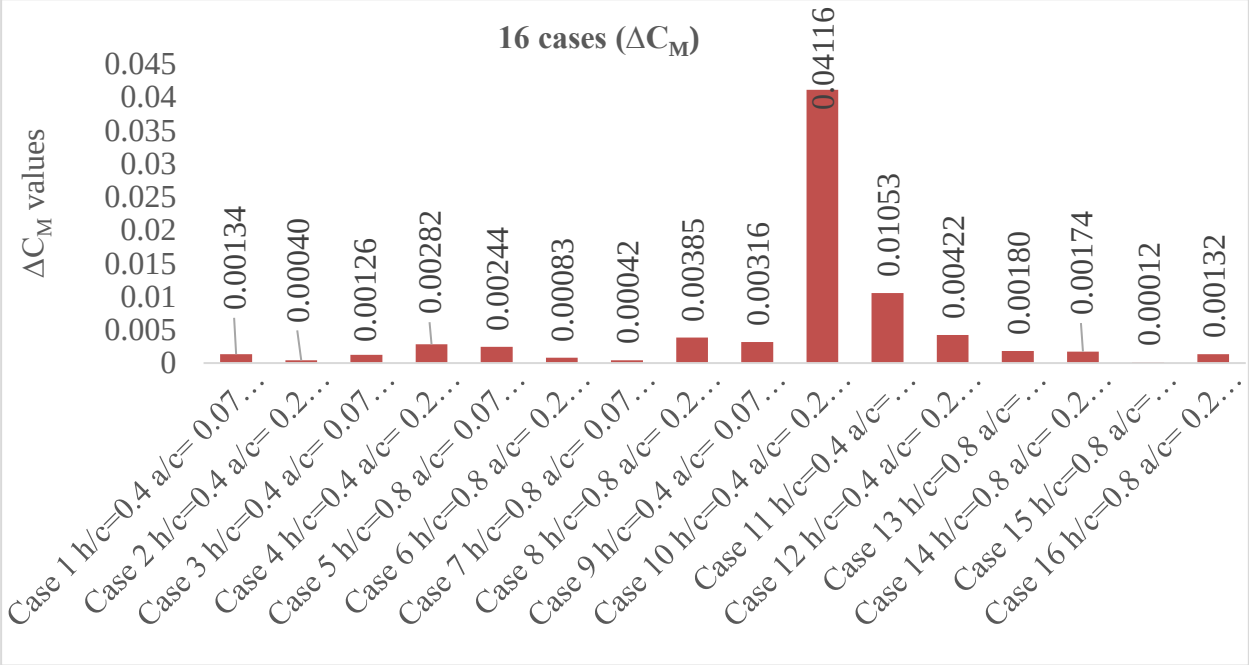

Figure 14. Comparison of C_M values with fluctuations for all cases

The largest moment fluctuation occurred in case 10. Close to the ground, high wave amplitude and short wavelength cause large fluctuations in the moment value. Apart from this, it is understood that the moment fluctuation is slightly affected by all parameters. It can be said that the moment fluctuation decreases as the angle of attack decreases, as it moves away from the ground, and at low wave amplitudes.

The beta value (β) is defined as the ratio of the difference between the maximum and minimum values of the moment coefficient (C_M) to the average moment coefficient and represents the moment variability of the system. The lower this β value, the more stable the system can be interpreted as in terms of moment.

$$\beta = \frac{C_{M,max} - C_{M,min}}{C_{M,avg}} \quad (7)$$

The β value reflects the variability of the moment coefficient and the tendency of the system to instability. If the value is large, it indicates that the moment coefficient varies more than the average value, and therefore the system can oscillate more.

In the literature, aerodynamic stability and unstable behavior are generally evaluated using metrics such as the mean moment coefficient, peak-to-peak moment variation, or the root mean square value of the moment coefficient [2]. While these indicators provide valuable information, they are usually dependent on the absolute magnitude of the aerodynamic loads. In contrast, the proposed β metric allows for a relative and dimensionless assessment of moment variability by normalizing the moment fluctuation with the mean moment coefficient. This normalization makes β particularly suitable for comparative evaluations under different operating and ground effect conditions where absolute moment levels may vary. A normalized interval-based indicator similar to the existing β metric has previously been used to measure the amplitude of fluctuations in aerodynamic coefficients. In this study, the metric β is defined as a normalized measure of fluctuations in the moment coefficient. In similar studies in the literature [3], the normalized maximum-minimum difference of the aerodynamic coefficients according to time-averaged values has been used to comparatively evaluate the fluctuation amplitude. This study provides a unique contribution to the literature by applying this approach to the moment coefficient for the first time and presenting a systematic comparison under different wave parameters.

The distribution of β values is shown in Figure 15 with a different graph. As a result, low h/c, low λ/c, and high a/c ratios increase moment variability at both 0° and 8° angles of attack, triggering system instability. In this context, if high stability is aimed, it is recommended to prefer high h/c and λ/c ratios. In addition, the moment variability is generally higher at 8° AOA than at 0° AOA, indicating that angle of attack is also an important parameter on instability.

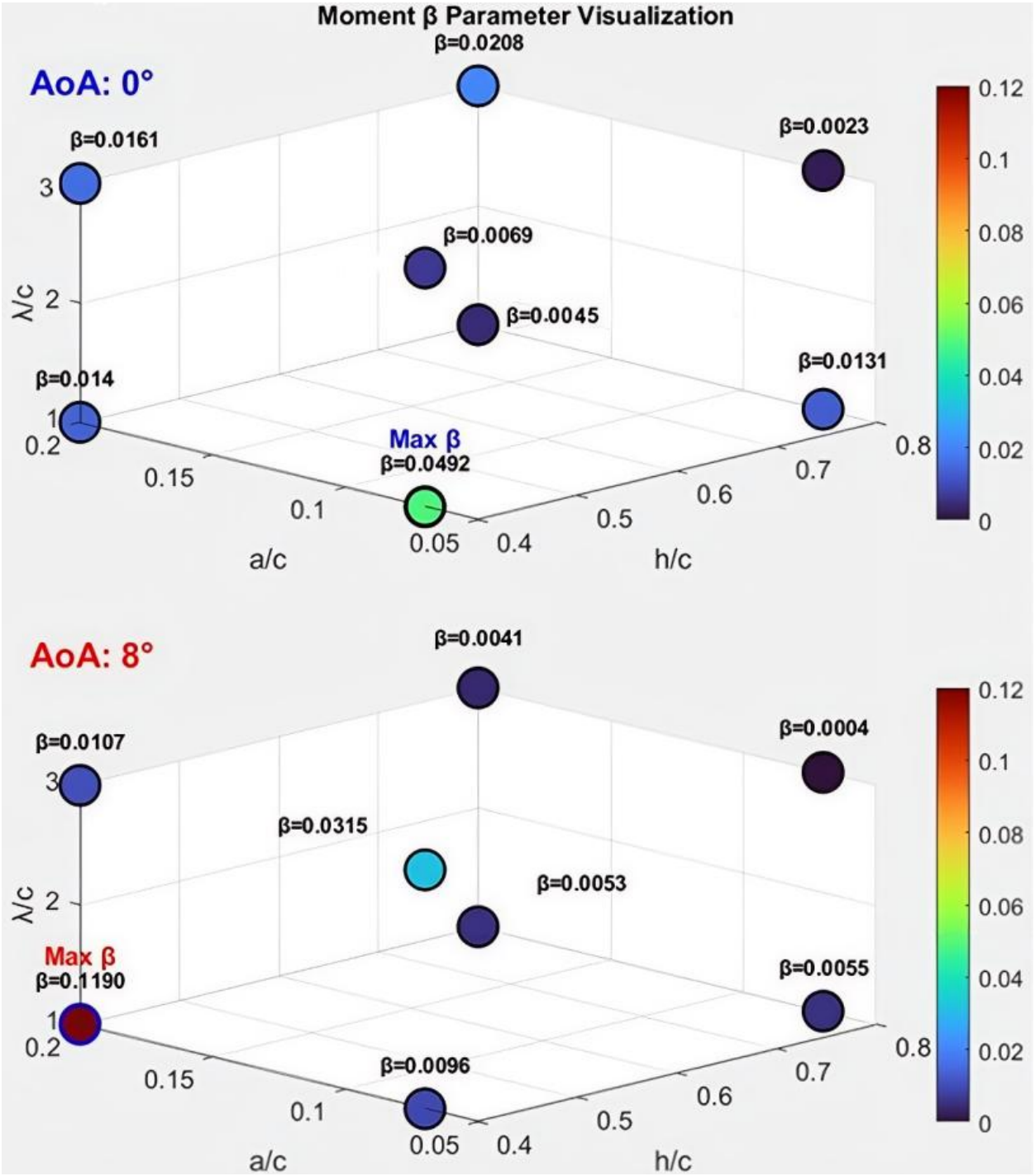

Figure 15. Comparison of the β stability metric (C_M fluctuation range normalized by the mean C_M) in all cases for 0° and 8°, lower β values indicate higher moment stability.

All the results for the lift, drag, moment and β as well, are changing with α, a/c, λ /c and h/c. When the angle of attack (α) is examined at values such as 0° and 8°: 0° angle of attack shows a different characteristic compared to 8° angle of attack. As the angle of attack increases, lift increase**,** moment change and drag increase are generally observed. The crest and trough regions of the wave

change the local pressure distribution, creating time-varying effects on lift and drag. As the distance between the airfoil and the surface increases, the ground effect weakens. In this case, the effect of the wave decreases and the flow becomes freer. As the airfoil is approached to the wavy surface, both the wave-induced fluctuation and the increase in lift value become apparent. This directly affects the stability of ekranoplan and WIG vehicles, in particular. As the amplitude increases, the effects on the flow become more pronounced. High amplitude waves increase undulation in the flow, creating instability, especially for small angles of attack. These results are summarized in Table 6.

Table 6. Summary of the effects of four different parameters on lift, drag and moment coefficient values

Parameters	**What happens if it increases?**
$\alpha \uparrow$	C_L, C_D and C_M increase; $\Delta C_L\uparrow$, $\Delta C_D\uparrow$ and $\Delta C_M\uparrow$
$h/c \uparrow$	The wave effect decreases; C_L and C_D do not change significantly; ΔC_L and ΔC_D are negligible; $\Delta C_M \downarrow$
$a/c \uparrow$	Fluctuations of ΔC_L, ΔC_D and ΔC_M increase; $\Delta C_L\uparrow$, $\Delta C_D\uparrow$, and $\Delta C_M\uparrow$
$\lambda/c \uparrow$	ΔC_L and ΔC_D fluctuate less, but the effect is also very dependent on other parameters; $\Delta C_M \downarrow$
$a/\lambda \uparrow$	$\Delta C_L\uparrow$, $\Delta C_D\uparrow$ and $\Delta C_M\uparrow$

These findings provide important data for improving aerodynamic performance, especially in systems designed for ground effect vehicles (WIGs) or low-altitude flights.

4. CONCLUSION

In this study, the time-dependent effects on the lift (C_L), drag (C_D), and moment (C_M) coefficients of a NACA 4412 airfoil moving on a wavy ground were calculated using the URANS equations. The analyses revealed the effects of critical parameters such as AOA, h/c, a/c and λ/c on aerodynamic performance and stability.

CFD results show that an increase in the angle of attack leads to significantly higher lift, drag, and moment coefficients, as well as larger wave-induced fluctuations in these coefficients. As the proximity to the ground increases, the results show that the lift force and C_L/C_D ratio increase, and the drag force tends to decrease. It has been determined that as the wavelength increases and the wave amplitude decreases, the fluctuation on the coefficients decreases. However, the effects of wave parameters (wavelength and amplitude) on the maximum and minimum values of the lift,

drag and moment coefficients differ, especially depending on the ground clearance and angle of attack. The ratio of wave amplitude to wavelength (a/λ) has a decisive effect on the temporal fluctuations of the coefficients, and as this ratio increases, the magnitude of the fluctuations in the coefficients also increases.

The main observations of the study reveal the dominant effect of the angle of attack on the aerodynamic coefficients. At 8° AOA, both lift and drag coefficients showed much larger fluctuations than at 0° AOA. This suggests that the airfoil is more sensitive to surface waves while generating a significant amount of lift force. When the wave amplitude effect is examined, larger amplitudes (a/c=0.2) increase fluctuations, especially at 0° AOA, while at 8° AOA the effect is more inconsistent, but still noticeable. . The effect of wavelength, on the other hand, is variable; in some cases longer wavelengths increase fluctuations, in others decrease them, and according to the data, no clear universal trend has been detected. A higher ground clearance (h/c=0.8) improves stability by reducing fluctuations. The lower altitude (h/c=0.4) increased fluctuations, especially at 8° AOA. This suggests that greater proximity to the ground makes it more challenging to stabilize aerodynamic performance.

Although 8° AOA is preferred in scenarios that require the highest lift, this significantly increases drag in the wavy environment, leading to instability. optimal configuration for a stable flight; 0° AOA is a combination of h/c=0.8 (high altitude), λ/c=3 (long wavelength), and a/c=0.07 (small wave amplitude). This combination provides the smallest fluctuations in lift and drag forces, ensuring the most stable flight over wavy surfaces. Conversely, the combination of 8° AOA, h/c=0.4, λ/c=1 and a/c=0.2 (Case 12) represented the riskiest situation, with an extreme variation in the C_L/C_D ratio ranging from 33 to 45. High AOA cases (8°) show a strong sensitivity to wave parameters, leading to less stability. Therefore, low AOA (0°) may be preferred for stable operations on wavy surfaces.

This study is limited to two-dimensional simulations that neglect three-dimensional flow effects and vortex structures along the wingspan. Therefore, absolute aerodynamic coefficients may differ from full three-dimensional results. Besides, the drag and lift coefficients appear to be larger in two-dimensional case. However, the two-dimensional approach is sufficient to capture relative trends and comparative performance under varying ground effect conditions.

The study reveals that aerodynamic performance under wavy surface conditions is a complex and multidimensional problem. The effects of wave parameters on lift, drag and moment characteristics have made significant contributions to the development of CFD analysis methodologies. However, more research is needed in areas such as modeling three-dimensional

effects and validation studies in real operational conditions. Future studies should focus on the development of control strategies for practical applications, especially for large-scale WIG vehicles.

NOMENCLATURE

CFD	:	Computational Fluid Dynamics	h	:	Ground clearance
URANS	:	Unsteady Reynolds Averaged Navier Stokes	a	:	Wave amplitude
SST	:	Shear Stress Transport	AOA	:	Angle of Attack
Re	:	Reynolds	ρ	:	Air density
C_L	:	Lift coefficient	T	:	Period
C_D	:	Drag coefficient	t	:	Time
C_M	:	Moment coefficient	$C_L(t)$	:	Lift coefficient with time
C_P	:	Pressure coefficient	$C_D(t)$	:	Drag coefficient with time
L	:	Lift force	$C_M(t)$	:	Moment coefficient with time
D	:	Drag force	CFL	:	Courant-Friedrichs-Lewy
M	:	Moment	Δt	:	Time step size
c	:	Airfoil chord length	α	:	Angle of attack
A	:	Reference area	β	:	Beta (stability metric)
V	:	Free stream velocity	SAS	:	Scale-Adaptive Simulation
λ	:	Wave length	y^+	:	Y plus

DECLARATION OF ETHICAL STANDARDS

The authors of the paper submitted declare that nothing which is necessary for achieving the paper requires ethical committee and/or legal-special permissions.

CONTRIBUTION OF THE AUTHORS

Mehmet Bakırcı: The conceptual design of the study was developed. The CFD model setup, including mesh generation and boundary conditions, was prepared. The numerical simulations and post-processing of the results were carried out. The interpretation of aerodynamic performance parameters was performed collaboratively. The literature review and identification of research gaps were conducted. The visualization of CFD contours was prepared. The discussion and

comparison with previous studies were mainly written. The computational resources and simulation environment were managed.

Muhammed Islam: The experimental data used for validation were collected and organized. The literature review was conducted. The development of figures, tables, and graphical abstracts was completed. The proofreading, editing, and English language correction of the manuscript were performed.

CONFLICT OF INTEREST

There is no conflict of interest in this study.

REFERENCES

[1] Rozhdestvensky K V. Wing-in-ground effect vehicles. Progress in Aerospace Sciences 2006; 42(3): 211–283.

[2] Qu Q, Lu Z, Liu P, Agarwal RK. Numerical study of aerodynamics of a wing-in-ground-effect craft. Journal of Aircraft 2014; 51(3): 913–924.

[3] Hu H, Ma D. Airfoil aerodynamics in proximity to wavy ground for a wide range of angles of attack. Applied Sciences (Switzerland) 2020; 10(19).

[4] Liu X, Ma D, Yang M, Guo Y, Hu H. Numerical study on airfoil aerodynamics in proximity to wavy water surface for various amplitudes. Applied Sciences 2021; 11(9), 4215.

[5] Su Y, Li D, Zhao S. Lift augmentation of a circulation control airfoil in proximity to water waves. Journal of Physics: Conference Series, Beihang University, Beijing, China, 2024; 2913(1), 012012.

[6] Qu Q, Jia X, Wang W, Liu P, Agarwal RK. Numerical study of the aerodynamics of a NACA 4412 airfoil in dynamic ground effect. Aerospace Science Technology 2014; 38: 56–63.

[7] Firooz A, Gadami M. Turbulence flow for NACA 4412 in unbounded flow and ground effect with different turbulence models and two ground conditions: Fixed and moving ground conditions. Int. Conference on Boundary and Interior Layers (BAIL 2006), Göttingen, Germany, 2006.

[8] He W, Guan Y, Theofilis V, Li LKB. Stability of low-Reynolds-number separated flow around an airfoil near a wavy ground. AIAA Journal 2019; 57(1): 29–34.

[9] Liang H, Zong Z, Zou L. Nonlinear lifting theory for unsteady WIG in proximity to incident water waves. Part 1: Two-dimension. Applied Ocean Research 2013; 43: 99–111.

[10] Win SY, Thianwiboon M. Parametric optimization of NACA 4412 airfoil in ground effect using full factorial design of experiment. Engineering Journal 2021; 25(12): 9–19.
[11] Nebylov A, Nebylov V, Fabre P. WIG-Craft flight control above the waved sea. IFAC Conference Papers on Line 2015; 48(9); 102–107.
[12] Matdaud Z, Zhahir A, Pua'At AA, Hassan A, Ahmad MT. Stabilizing attitude control for mobility of wing in ground (WIG) craft - A Review. IOP Conference Series: Materials Science and Engineering. Institute of Physics Publishing 2019, 705(1), 012038 (Presented at the 5th International Conference on Mechanical, Automotive and Aerospace Engineering 2019).
[13] Cui, E., & Zhang, X. (2007). Ground effect aerodynamics. In C. Tropea, A. L. Yarin, & J. F. Foss (Eds.), Springer Handbook of Experimental Fluid Mechanics Springer, 2007; 721–748.
[14] Smuts EM, Sayers AT. CFD study of a wing in close proximity to a flat and wavy ground plane. R & D Journal of the South African Institution of Mechanical Engineering 2011; 27: 1-9.
[15] Ahmed MR, Takasaki T, Kohama Y. Experiments on the aerodynamics of a cambered airfoil in ground effect. In: Collection of Technical Papers - 44th AIAA Aerospace Sciences Meeting. American Institute of Aeronautics and Astronautics Inc. 2006; 3132–3148.
[16] Castelli M R, Englaro A, Benini E. The Darrieus wind turbine: Proposal for a new performance prediction model based on CFD. Energy 2011; 36(8): 4919-4934.
[17] Du P, Agarwal RK. Drag prediction of NASA common research models using different turbulence models. American Institute of Aeronautics and Astronautics (AIAA) 35th AIAA Applied Aerodynamics Conference, AIAA Aviation Forum, Denver, CO, United States. AIAA, 2017; Paper 2017, 3560.